(Received 31 December 2025, Accepted 11 February 2026, Scheduled 10 March 2026)

Energy Efficiency Maximization for IRS-Assisted UAV-D2D Cooperative MEC Offloading

Chenwei Feng*, Haojun Xing, Jun Zhou, Zhenzhen Lin, Huangjie Guo, and Ruilong Chen

School of Opto-Electronic and Communication Engineering, Xiamen University of Technology, Xiamen 361000, China

ABSTRACT: With the rapid development of technologies, such as Big Data, Cloud Computing, Artificial Intelligence (AI), and the Internet of Things (IoT), there is an increasing demand for real-time computing and low-latency data transmission. Mobile Edge Computing (MEC) technology has been proposed to reduce data transmission latency and alleviate the burden on the core network; however, MEC still faces the problem of limited computational resources and bandwidth in high-density device environments. To address these issues, this study proposes a joint optimization energy-efficiency maximization strategy for Intelligent Reflective Surface (IRS)-based unmanned aerial vehicle (UAV) and device-to-device (D2D) collaborative Mobile Edge Computing (MEC) systems. The strategy integrates the optimization of task offloading decisions, UAV trajectory planning, computational resource allocation, and IRS phase regulation to maximize the system's energy efficiency. The highly coupled and non-convex optimization problem is solved iteratively by designing a two-loop iterative optimization framework that combines Dinkelbach's algorithm with the block coordinate descent (BCD) method, utilizing the Lagrange multiplier method and the successive convex approximation (SCA) technique. Simulation results show that the optimization strategy in this study significantly improves the energy efficiency of the system compared to the conventional scheme, especially in IRS phase optimization and UAV trajectory adjustment.

1. INTRODUCTION

With the rapid development of technologies, such as big data, cloud computing, artificial intelligence (AI), and the Internet of Things (IoT), the demand for information processing and data transmission continues to grow. Application scenarios, such as smart cities, Industrial Internet of Things (IIoT), and intelligent transport require real-time computation and decision-making on massive amounts of data to ensure the efficient operation of the system. However, it is difficult for the traditional cloud computing model to meet the demand for low latency and high computational efficiency in these applications because of high computational latency caused by long data transmission distances and core network congestion [1]. Therefore, Mobile Edge Computing (MEC) has emerged, which enables computational tasks to be processed in close proximity by deploying edge computing servers near wireless access points (APs) or base stations (BSs), effectively reducing data transmission latency while reducing the computational load on the core network.

Although MEC can mitigate the high latency issues of cloud computing to some extent, the computational resources and bandwidth remain constrained, particularly in high-density device environments. Competition for computational resources and communication bottlenecks resulting from task offloading remains a significant challenge. To address these challenges, unmanned aerial vehicles (UAVs) can serve as vital complements to MEC systems because of their high maneuverability and flexible deployment capabilities. When equipped with MEC servers and UAVs can rapidly cover signal blind spots and computationally intensive areas. By collaborating with ground base stations, UAVs enhance their computational capacity to meet peak-hour computing demands. However, an important factor to consider is the energy cost of drones for transmitting and processing information. To minimize the energy consumption of drones, multiple tasks should be appropriately offloaded to other devices. Therefore, device-to-device (D2D) communication was introduced into the MEC architecture. Direct data interaction between devices is enabled. As a result, reliance on edge servers is reduced. The network load was also reduced. In addition, the transmission latency was effectively decreased. However, in complex wireless environments, D2D communication is susceptible to channel fading, interference, and coverage limitations, all of which affect the performance of MEC task offloading. Therefore, introducing Intelligent Reflective Surfaces (IRS) into MEC can effectively address propagation environment challenges. An IRS, or reconfigurable intelligent surface (RIS), consists of a large number of tunable passive reflecting elements. By dynamically adjusting the reflection phases, the directional reflection of signal beams can be achieved. Consequently, the quality os D2D communication is enhanced, and the reliability and efficiency of MEC task offloading are improved [2]. As an emerging wireless communication enhancement technology, IRS has garnered significant attention for optimizing MEC and D2D communications owing to its ability to intelligently adapt to wireless signal propagation environments [3].

The integration of UAVs and MEC systems has garnered increasing attention recently, with a focus on enhancing resource

* Corresponding author: Chenwei Feng (cwfeng@xmut.edu.cn).

allocation and task offloading efficiency. In the study of communication aided by a single UAV, the use of UAVs equipped with IRS panels as mobile base stations has been demonstrated [4] to enhance communication coverage and transmission reliability. To minimize the overall system latency, this study proposes a joint optimization framework that balances the power allocation, phase-shift control of the IRS, and UAV positioning. The use of UAVs enables dynamic adaptation to environmental changes, particularly in complex urban environments, where traditional communication infrastructure struggles to provide reliable coverage. However, the research only considered collaboration between the IRS and a single drone without accounting for multi-drone coordination scenarios, leaving room for improvement in system performance. To further enhance the communication modes of UAV-assisted networks, researchers have begun exploring the integration of UAV and D2D communications. The synergistic integration of UAV and D2D communications has been investigated [5], in which a collaborative UAV-assisted MEC framework was developed. Researchers have highlighted the value of D2D communication for offloading computational tasks to idle devices, thereby alleviating the computational burden on UAV-based MEC servers. The framework ensures the shortest task completion time through joint power allocation and offloading decisions, particularly when the UAV resources are limited. Further work will emphasize the need for the careful management of task allocation between UAVs and D2D devices to achieve optimal system performance. Physical layer security was investigated [6] for a cache-enabled UAV relay network with D2D communication, where both the UAV and selected UEs are equipped with caching capabilities. However, the hybrid offloading strategy in this research requires multiple iterations of the algorithm, resulting in high computational complexity, which may compromise the real-time communication performance. An iterative scheme for energy-efficient resource allocation in UAV-underlaid D2D communications was proposed [7]. The solution aims to optimize the overall energy efficiency of all D2D pairs while ensuring the quality of service requirements and confidentiality rates for all users. A novel method for managing resource allocation in multi-mobile UAV-D2D communications was proposed [8]. The formulated optimization problem aims to maximize energy-saving utility by considering power and bandwidth constraints in addition to associated limitations. A resource allocation strategy for UAV-D2D-assisted multi-relay MEC systems with energy-harvesting capabilities was presented [9]. This strategy addresses challenges such as the inability of devices outside the BS edge to offload tasks and the excessive burden of relay communication.

In scenarios involving multiple UAVs or multiple IRSs, the coordinated deployment of multiple UAVs and multiple IRSs further enhances network performance. A communication scenario supported by multiple UAVs equipped with onboard IRS for ultra-reliable low-latency communication (URLLC) is investigated [10]. In this scenario, each UAV acts as a repeater, reflecting signals from the macro-base station to users located far from the base station. A joint optimization problem was developed to optimize UAV deployment, base station power allocation, IRS phase adjustment, and the length of URLLC transmission blocks. Given the complex non-convex nature of the problem, the solution is obtained by applying a deep neural network (DNN) algorithm. The simulation results demonstrate that aerial RIS technology has significant potential for supporting stringent URLLC requirements. The significant potential of aerial IRS for enhancing the coverage of massive multiple-input multiple-output (mMIMO) networks has been demonstrated [11]. An optimization model was created to maximize network throughput by adjusting the power allocation of the base station (BS) and phase control coefficients of multiple in-building repeaters (IRSs). Iterative algorithms were used to solve this problem, demonstrating that IRS can effectively enhance the overall network throughput while improving the performance of the worst-case user. Compared to other baseline approaches, the IRS also exhibits lower computational complexity. However, IRS lacks transmitting-receiving links, making channel information (CSI) acquisition challenging for certain paths. In most cases, deploying a large number of metasurfaces for IRS increases the channel size and time required to obtain CSI [12]. Therefore, the issue of precise CSI acquisition in the IRS technology cannot be overlooked.

Combining key technologies in pairs greatly increases the potential functionality of MEC systems through synergistic optimization across various technologies. The integration of UAV and MEC has shown significant research advantages. A scenario in which the UAV serves as a flying base station (BS) equipped with an MEC server (UAV-MEC) was proposed [13]. To minimize the total delay experienced by user devices, researchers have designed an iterative algorithm to jointly optimize the user association, transmission power, and computational resource allocation. Experimental results demonstrate that compared to traditional orthogonal frequency division multiple access (OFDMA) systems, UAV-MEC systems employing non-orthogonal multiple access (NOMA) technology exhibit significant advantages in reducing communication latency and enhancing overall system performance. Furthermore, the introduction of IRS significantly improves the task offloading performance in MEC systems. An RIS-assisted MEC system for heterogeneous networks (HetNet) has been proposed [14]. To minimize the total latency of the system, a joint optimization problem was formulated by optimizing the allocation of caching, task offloading, and computational resources. Because the problem is NP-hard, a two-stage optimization algorithm was proposed for the solution. Simulation results indicate that compared to the approach without RIS, the introduction of RIS can significantly reduce task processing delays and enhance the overall system performance. Finally, regarding the collaborative optimization of RIS and UAV, a RIS-enhanced UAV-MEC framework was studied [15]. Within this framework, the UAV is deployed statically, and communication is enhanced between the RIS and ground access point (AP). A two-step optimization algorithm was developed to simultaneously optimize the RIS phase control, communication computational resource allocation, and decoding sequence. The simulation results show that the proposed scheme effectively enhances the computational capability of the system, demonstrating significant performance improvements compared to existing approaches. A system model with a UAV serving as a relay

node was further investigated [16], where the UAV's flight trajectory could be dynamically adjusted to enhance task offloading performance. A joint optimization algorithm was proposed to compute the unloading task, RIS phase control, bandwidth allocation, and UAV flight trajectory. The simulation results show that RIS and NOMA technologies play critical roles in optimizing UAV trajectories, significantly improving the computational capability and network performance of the system. While existing research has achieved important breakthroughs in MEC, D2D communication, and IRS technologies, most efforts have focused on optimizing these technologies separately, lacking systematic research on their coordinated optimization.

While significant progress has been achieved in the research on MEC, D2D communications, and IRS, these technologies have primarily been investigated in isolation or in pairs. A systematic investigation into the collaborative optimization of all three technologies has yet to be conducted. In the current 5G and upcoming 6G network environments, the rapid growth in the number of smart devices has driven a continuous rise in user demand for low-latency, high-reliability computing services. By deploying computing resources at the network edge, MEC effectively reduces the data backhaul latency to the core network, thereby significantly enhancing the overall computing efficiency. However, the service coverage and processing capacity of traditional MEC systems are limited by the deployment density and resource scale of the ground-based infrastructure [17]. In high-rise dense urban environments or areas with infrastructure damaged after disasters, the service capabilities and network stability of such systems still face significant challenges. To address the aforementioned challenges, emerging technologies, such as D2D communication, IRS, and UAVs, have been incorporated into the MEC architecture in recent years to synergistically improve system performance. D2D communication enables direct data transmission between end devices, effectively reducing the transmission latency and alleviating the load on the edge servers. IRS achieves signal path reconstruction and enhancement by regulating the phase of a large number of passive reflective units, improving the channel quality, and lowering the communication latency. As highly maneuverable aerial MEC nodes, UAVs offer flexible deployment advantages, enabling the rapid coverage of resource-scarce ground areas to provide computing and communication support. Simultaneously, UAVs can serve as relay nodes to extend coverage and enhance the stability of D2D communication [18].

Currently, MEC systems based on IRS and D2D have achieved preliminary multi-dimensional resource coordination optimization for communication, computing, and coverage resources, demonstrating excellent performance in high-density networks. However, existing research primarily focuses on network configurations with static or semi-static deployments. In real-world environments with physical obstructions or insufficient IRS deployment, the communication efficiency of D2D links remains susceptible to degradation in channel quality. While IRS can enhance signal quality through passive beamforming, performance remains highly dependent on acquiring channel state information and location data, severely limiting IRS accuracy in dynamic, complex environments. Therefore, further integrating UAVs into the IRS-D2D-MEC architecture not only enables dynamic aerial resource deployment and coverage enhancement through their high mobility but also expands the task offloading scope for D2D devices and alleviates computational pressure on ground nodes by deploying UAV-mounted MEC servers or utilizing UAVs as relay nodes. Moreover, the introduction of UAVs facilitates the establishment of air-ground collaborative scheduling capabilities. By enabling joint optimization of task offloading, resource allocation, and trajectory planning in complex environments, this approach enhances system adaptability and reliability when addressing sudden tasks, physical obstructions, and network topology changes.

Based on the aforementioned challenges, an IRS-assisted D2D-MEC collaborative offloading optimization strategy is proposed. The strategy aims to optimize task offloading, computing resource allocation, and wireless channel quality, with the goal of minimizing the overall system latency and enhancing computational energy efficiency. The contributions of this study are summarized as follows.

Construction of IRS-assisted UAV-D2D collaborative MEC system architecture: This paper proposes a new MEC collaborative offloading architecture that integrates IRS, UAV, and D2D communication technologies, comprehensively considering the channel gain enhancement effect of IRS on the wireless link, as well as the advantages of flexible deployment of UAVs and high mobility, and constructs a multi-mode task offloading mechanism, which effectively solves the problem of communication bottlenecks and insufficient computational resources in task offloading in high-density environments. The problems of communication bottlenecks and insufficient computational resources for task offloading in high-density environments are effectively solved.

Dual-loop iterative optimization framework based on the Dinkelbach method: To solve the non-convexity and multivariate coupling problems of the energy efficiency optimization problem, this paper designs a dual-loop iterative optimization framework that combines the Dinkelbach algorithm and block coordinate descent (BCD). In the outer loop, the Dinkelbach method is used to transform the energy-efficiency fractional planning problem into an equivalent subtractive form; in the inner loop, the BCD method is used to decompose the original optimization problem into three sub-problems: offloading mode selection and task allocation optimization, joint optimization of the UAV trajectory and computational resources, and optimization of the IRS phase beamforming and solve them alternately, which effectively reduces the algorithmic complexity and ensures convergence.

Joint optimization algorithms: In this study, a joint optimization algorithm is proposed to combine the task offloading decision, UAV trajectory optimization, resource allocation, and IRS phase beamforming. The offloading mode and offloading ratio are optimized alternatively to ensure high efficiency of task offloading, the UAV trajectory and computational resource allocation are optimized by the gradient descent method to minimize the energy consumption, while the IRS phase is optimized by the Successive Convex Approximation (SCA) method to

improve the quality of the signal transmission and the overall improvement of the energy efficiency of the system. This integrated optimization approach effectively solves the multivariate coupling problem and enhances the computational and communication performance of the system.

The rest of the paper is organized as follows. Section 2 establishes the system model and problem formulation. Section 3 provides a detailed decomposition of the mathematical formulation of the problem and the optimization problem, and elaborates on the specific implementation process of the proposed algorithms, including task offloading decision-making and allocation, UAV trajectory and resource optimization, and IRS phase optimization methods. Section 4 validates the superiority of the proposed methods through simulation analysis. Section 5 concludes the paper.

2. SYSTEM MODELING AND PROBLEM FORMULATION

In this paper, we propose an IRS-based MEC offloading architecture for UAV and D2D communication convergence, which supports two modes of task offloading for user devices (UDs): one is to provide computation services for UDs through the MEC server carried by the UAV, and the other is to offload computation tasks to the neighboring idle UDs using the D2D communication link. This architecture effectively improves the wireless link quality through IRS-assisted communication, and meets the low-latency and high-reliability requirements in dense device scenarios. Figure 1 illustrates an IRS-based UAV-D2D collaborative MEC task offloading system. The system comprises a cellular access network and a D2D communication network, a UAV equipped with an edge server, UDs, service equipment (SeDs), and an IRS with N reflectors. UAV flies at a fixed altitude H, serving as an MEC server to provide communication and computing services for multiple UDs. Dotted lines indicate invalid communication links between UDs obstructed by obstacles along the propagation path, while solid lines represent valid communication links established between UDs and the UAV/SeDs via IRS reflection. UDs possess limited computational resources and must execute delay-sensitive, computationally intensive tasks. The SeDs consist of idle users with relatively high computational capabilities, which remain limited compared to edge servers and cannot simultaneously handle multiple computationally intensive tasks. Define $\mathcal{M} = \{1, 2, \ldots, \mathbf{M}\}$, $\mathcal{K} = \{1, 2, \ldots, K\}$, and $\mathcal{N} = \{1, 2, \ldots, N\}$ as the set of UDs, SeDs, and reflective elements of the access system, respectively. Assume that the system operates over a specified mission period T, divided into time slots I and indexed as $\mathcal{I} = \{1, 2, \ldots, I\}$. The time slot length $\delta_i = \frac{T}{I}$ is sufficiently small such that the UAV flies over a small distance in each time slot with a roughly constant channel gain.

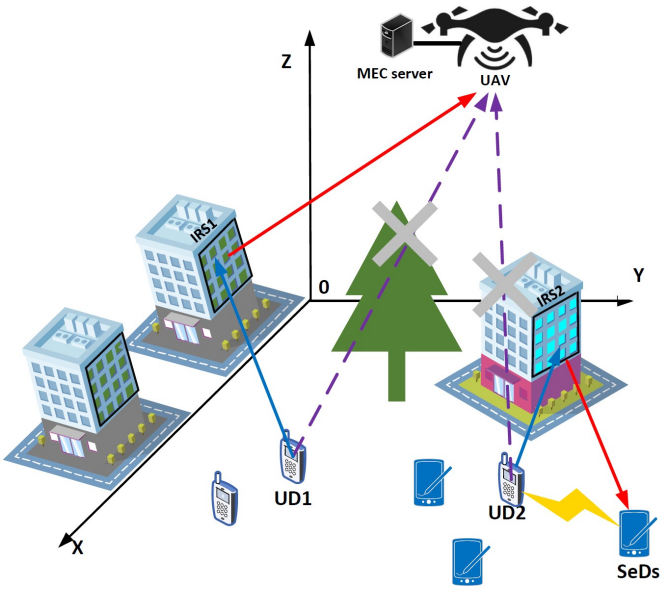

FIGURE 1. Model of UAV-D2D collaborative MEC mission offloading system with IRS.

2.1. Communication Model

The height of the UDs is zero, and for the mth UE, its coordinates can be denoted as $\mathbf{z}_m = (X_m, Y_m)$. Similar to [12] and [14], it is assumed that the UAV flies at a fixed altitude $H > 0$. The horizontal position and height of the first cell on an IRS with a uniform linear array (ULA) are given by $\mathbf{z}_R = (X_R, Y_R)$ and h_R, respectively. Using the IRS, a virtual LoS connection between UAVs and UDs can be achieved by adjusting the phase shift of the IRS. Because the phase shift of each reflection element of the IRS can be dynamically adjusted by the controller, the amplitude reflection coefficients of all reflection units are set to 1, and the vector of phase shift coefficients of the first IRS is by $\theta^{(l)} = [\theta_1^{(l)}, \theta_2^{(l)}, \ldots, \theta_N^{(l)}]^T$, where, for all $n \in \{1, 2, \ldots, N\}$, $\theta_n^{(l)} \in [0, 2\pi)$, then the lth IRS reflection coefficient matrix $\mathbf{\Theta}^{(l)} = \text{diag}\{e^{j\theta_1^{(l)}}, e^{j\theta_2^{(l)}}, \ldots, e^{j\theta_N^{(l)}}\}$ is obtained, where j represents the imaginary unit, and let $\mathbf{\Phi} = \mathbf{\Theta}^{(1)}, \mathbf{\Theta}^{(2)}, \ldots, \mathbf{\Theta}^{(L)}\}$ denote the set of phase variables for all L IRSs. Set $\mathbf{x} = \{x_1, x_2, \ldots x_m, \ldots, x_M\}, \forall m \in \mathcal{M}$ to denote the offloading mode selection of the UDs. Let $x_m = 1$ denote that the mth UD uses the UAV-based offloading mode, and vice versa, and $x_m = 0$ denotes that the UDs use the D2D distributed computing offloading mode.

2.1.1. UAV-Based Offloading

Consider a communication system composed of Q UDS, K IRS, and UAV-MEC server. The kth UAV detects a UDs message in the time slot and generates the corresponding perception data. Definition: The binary variable $A_{m,l}$ indicates whether UD_m has been assigned to the lth IRS. Specifically, $A_{m,l} = 1$ signifies that UD_m has been assigned to the lth IRS. $A_{m,l} = 0$ indicates that UD_m has not been assigned to the lth IRS; each UD_m is assigned to only one IRS. We define the binary variable $R_j \in [0, 1]$ to indicate whether the MEC server receives an external request in time slot j. Upon receiving a request $R[j]$, the MEC server verifies the validity of the UD_m unique identifier. If valid, the server immediately assigns a channel and establishes a transmission path. If invalid, the server reexamines the request and continues with the verification process.

Assuming that the system operates for a specified mission period T, which is divided into I time slots, and I is

sufficiently large, then δ_i is sufficiently small such that the UAV flies a small distance, the position remains approximately constant, and the channel gain remains approximately constant within each time slot, as described in the literature [19]. The position of its flight phase can be denoted as $\mathcal{Z}^{\mathrm{U}} = \{z_1^{\mathrm{U}}, z_2^{\mathrm{U}}, \ldots, z_i^{\mathrm{U}}, \ldots z_I^{\mathrm{U}}\}$. For time slot i, the coordinates of the UAV are denoted as $\mathbf{z}_i^{\mathrm{U}} = (X_i^{\mathrm{U}}, Y_i^{\mathrm{U}})$. Velocity v_t can be obtained from the displacement in the time interval δ_i, and acceleration v_t^a can be obtained from the difference in velocities between two consecutive time slots. Then, the following can be obtained:

$$\nu_i = \frac{\left\|\mathbf{z}_i^{\mathrm{U}} - \mathbf{z}_{i-1}^{\mathrm{U}}\right\|}{\delta_i}, \tag{1}$$

$$v_i^a = \frac{v_i - v_{i-1}}{\delta_i}. \tag{2}$$

In the UAV-assisted mission offloading mode of this study, owing to the long communication distance between UAVs and UDs, the system adopts Orthogonal Frequency Division Multiple Access (OFDMA) for data transmission to improve the spectrum utilization and enhance the anti-jamming capability. In the D2D offload mode, owing to the smaller communication range and higher transmission rate between devices, the system also adopts OFDMA to ensure that multiple devices can communicate efficiently and in parallel; thus, the communication link for task offloading can more stably support concurrent transmissions from multiple users while improving the system's computational offloading efficiency and spectrum utilization. Furthermore, the IRS enhances the signal of the target user while suppressing interference from other users through spatial beamforming. By implementing these techniques, the system can achieve efficient communication and computation offloading while supporting data transmission from multiple UDs in each time slot without interfering with each other [20]. This approach effectively manages communication and resource utilization to enable collaborative computation and communication between the active and idle devices. In the UAV-based offloading model, multiple UDs can upload data within each time slot. Each UD is allocated a specific transmission time within a time slot to offload its tasks to the server. Considering the IRS-assisted communication system, the computational model associated with the IRS is introduced next. Specifically, for any time slot i, the distance between the UAV and first IRS is

$$d_{RU} = \sqrt{(H - h_R)^2 + \left\|\mathbf{z}_i^{\mathrm{U}} - \mathbf{z}_R\right\|^2}. \tag{3}$$

Because the UAV is flying at a high altitude, and the IRS is placed on the facade of a building, the communication link between the UAV and the lth IRS is assumed to be an LoS channel. Therefore, for any time slot i, the channel gain between the UAV and IRS can be given by the following equation:

$$\mathbf{h}_{R,U} = \sqrt{\rho {d_{RU}}^{-2}} \left[1, \ldots, e^{-j\frac{2\pi}{\lambda}(N-1)d\varphi_{IU}}\right], \tag{4}$$

where ρ is the path loss at the reference point $D_0 = 1\,\mathrm{m}$; d is the antenna spacing; λ is the carrier wavelength; and $\varphi_{\mathrm{RU}} = (X_R - X_i^U)/d_{RU}$ denotes the cosine of the angle of departure (AoD) of the signal from the lth IRS to the UAV at any time slot i.

It is assumed that the direct link from the UDs to the UAV is blocked by obstacles [15, 16]. Therefore, for any time slot t, the channel gain from the mth UD (UD_m) to the UAV can be expressed as:

$$\mathbf{h}_{m,U} = \sqrt{\rho {d_{\mathrm{mU}}}^{-\varepsilon}} g_{m\mathrm{U}}, \tag{5}$$

where $d_{mU} = \sqrt{\|\mathbf{z}_m - \mathbf{z}_i^U\|^2 + H^2}$ is the distance between the UAV and UD_m for any moment i; ε is the path loss exponent; and $g_{m\mathrm{U}}$ is a random variable following a circularly symmetric complex Gaussian distribution with mean zero and unit variance.

Communication links from UD_m to the lth IRS are assumed to be Rice channels [15], consisting of LoS and non-LoS (NLoS) components. Therefore, for any time slot i, the channel gain between UD_m and the lth IRS can be given by the following equation

$$\mathbf{h}_{m,R} = \sqrt{\rho d_{\mathrm{mR}}^{-\gamma}} \left[\sqrt{\frac{\beta}{1+\beta}}\mathbf{h}_{\mathrm{mR}}^{\mathrm{LoS}} + \sqrt{\frac{1}{1+\beta}}\mathbf{h}_{\mathrm{mR}}^{\mathrm{NLoS}}\right] \tag{6}$$

where $d_{\mathrm{mR}} = \sqrt{\|\mathbf{z}_{\mathrm{m}} - \mathbf{z}_{\mathrm{R}}\|^2 + {h_R}^2}$ is the distance between UD_m and IRS; γ denotes the path loss index, β represents the Rice factor; and $\mathbf{h}_{\mathrm{mR}}^{\mathrm{LoS}}$ and $\mathbf{h}_{\mathrm{mR}}^{\mathrm{NLoS}}$ are the LoS and NLoS components, respectively. For $\mathbf{h}_{\mathrm{mR}}^{\mathrm{LoS}}$, we have

$$\mathbf{h}_{\mathrm{mR}}^{\mathrm{LoS}} = \left[1, e^{-j\frac{2\pi}{\lambda}d\varphi_{\mathrm{mR}}}, \ldots, e^{-j\frac{2\pi}{\lambda}(N-1)d\varphi_{\mathrm{mR}}}\right]^T \tag{7}$$

where $\varphi_{\mathrm{mR}} = (X_{\mathrm{m}} - X_R)/d_{\mathrm{mR}}$ is the cosine of the angle of arrival (AoA) of the signal from UD_m to the IRS. The NLoS and $\mathbf{h}_{\mathrm{mR}}^{\mathrm{NLoS}}$ is a complex Gaussian distributed variable with zero mean and unit variance.

For any time slot i, the combined channel gain from UD_m to the UAV is given by the following equation:

$$h_m^U = h_{m,U} + (\mathbf{h}_{m,R})^H \boldsymbol{\Theta}^{(l)} \mathbf{h}_{R,U} \tag{8}$$

Let $p_{m,i}$ denote the transmitting power of UD_m, given a fixed bandwidth B^U and noise power σ^2 based on the UAV offloading. The offloading rate between UD_m and UAV can be expressed as

$$R_{m,i}^U = B^U \log_2\left(1 + \frac{p_{m,i}\left|h_m^U\right|^2}{\sigma^2}\right) \tag{9}$$

2.1.2. D2D Co-Offloading

In the D2D offloading model, the UDs offload tasks to the SeDs for processing. The channel coefficients from UD_m to the kth SeD (SeD_k), from UD_m to the lth auxiliary D2D IRS, and from the lth auxiliary D2D IRS to SeD_k are given as $h_{m,k} \in \mathbb{C}^{1\times 1}$, $\mathbf{h}_{m,k}^R \in \mathbb{C}^{N\times 1}$, and $\mathbf{G}_{d2d} \in \mathbb{C}^{N\times 1}$, respectively.

The combined channel gain from UD_m to SeD_k can then be expressed by the following equation:

$$h_{m,k} = h_{m,k} + (\mathbf{G}_{d2d})^H \mathbf{\Theta}^{(l)} \mathbf{h}^R_{m,k} \tag{10}$$

For any time slot i, given a fixed-bandwidth B^D and noise power σ^2_{d2d} in D2D offloading, the offloading rate between UD_m and SeD_k can be expressed as:

$$R^D_{m,i} = B^D \log_2 \left(1 + \frac{p_{m,i} |h_{m,k}|^2}{\sigma^2_{d2d}}\right). \tag{11}$$

2.2. Computational Model

To utilize full granularity in task allocation and computational resources, we consider a partial offloading approach. Specifically, computational tasks can be divided into arbitrary sizes, and some of them can be offloaded to MEC servers or SeDs, whereas the rest are processed locally. A computational task on UD_m can be described as a positive tuple $\{L_m, C_m\}$, where L_m is the size of the task data (in bits) and C_m denotes the computational resources required to compute one bit of the task (measured in CPU cycles per bit). We define variable $\alpha_m \in [0, 1]$ as the proportion of partial task offloading for UD_m. Then, bit $(1 - \alpha_m)L_m$ is processed locally and bit $\alpha_m L_m$ is offloaded to a remote device for processing. In each time slot, UD_m can perform both local computation and task offloading simultaneously, and considering the limitation of the computational capacity of the UDs, we have

$$\frac{(1-\alpha_m)L_m C_m}{\delta_i} \leq f_m, \quad \forall m \in \mathcal{M}, \quad i \in \mathcal{I}, \tag{12}$$

where f_m denotes the local computing power of UD_m measured in CPU cycles per second.

Similarly, f^U_m denotes the computational resources per second allocated by the UAV to UD_m for performing the offloading task, and the UAV computational resource allocation profile is defined as $F^U = \{f^U_m \mid m \in \mathcal{M}\}$. We have

$$\sum_{m=1}^{M} \frac{x_m \alpha_m L_m C_m}{\delta_i} \leq F^{\mathrm{U}}, \quad \forall i \in \mathcal{I}, \tag{13}$$

For the D2D-SeDs offloading part, SeDs are responsible for the computational processing of the task, and we have

$$\frac{\alpha_m L_m C_m}{\delta_i} \leq f_{mk}, \quad \forall m \in \mathcal{M}, \quad i \in \mathcal{I}, \tag{14}$$

where $f_{m,k}$ denotes the computational resources allocated by SeD_k to perform the offloading task at UD_m, such that $y_{m,k} = 1$ denotes that UD_m offloads the task to SeD_k, and vice versa $y_{m,k} = 0$. Subsequently, $\sum_{m=1}^{M} y_{m,k} \leq 1, \forall k \in K$ ensures that each SeD receives the offloading task from only one UD at a time.

Because the UAV can only count tasks that have been unloaded and received, we have

$$R^U_{m,i}\delta_i \geq \alpha_m L_m, \quad \forall m \in \mathcal{M}, \quad i \in \mathcal{I}. \tag{15}$$

2.3. Energy Consumption Model

2.3.1. UDs Calculate Energy Consumption

The local computational energy consumption of UD_m consists of two parts: task offload energy and local computational energy. First, the task offloading energy consumption of UD_m to UAV-MECs and SeDs at time slot i is $E^{\text{off,MEC}}_{m,i} = p_{m,i}\frac{\alpha_{\mathrm{m}} L_m}{R^U_{m,i}}$, $E^{\text{off,D2D}}_{m,i} = p_{m,i}\frac{\alpha_{\mathrm{m}} L_m}{R^D_{m,i}}$, respectively.

Then, owing to the offloading mode selection problem, the task offloading energy consumption of UD_m at time slot i can be expressed as

$$E^{\text{off}}_{m,i} = p_{m,i}\left[x_m \frac{\alpha_m L_m}{R^U_{m,i}} + (1 - x_m)\frac{\alpha_{\mathrm{m}} L_m}{R^D_{m,i}}\right], \tag{16}$$

Based on [18], the local computational energy consumed by UD_m at the ith time slot can be modelled as

$$E^{\text{com}}_{m,i} = \frac{\kappa_m \left[(1-\alpha_m) L_m\right]^3}{\delta_i^2}, \tag{17}$$

where κ_m is the effective capacitance factor of UD_m which depends on the architecture of the processor chip. Therefore, the total energy consumption of all the UDs of time slot i can be expressed as

$$E_{m,i} = \sum_{m=1}^{M} \left(E^{\text{com}}_{m,i} + E^{\text{off}}_{m,i}\right). \tag{18}$$

2.3.2. MEC Calculate Energy Consumption

Because the MEC server carries the UAV in the air, it provides computational services to the UDs. Under a model similar to that of the UDs, the computational energy consumption of the UAV in time slot i is

$$E^{\text{com}}_{\mathrm{U},i} = \sum_{m=1}^{M} \frac{\kappa_{\mathrm{UAV}} x_m \left(\alpha_m L_m\right)^3}{\delta_i^2}, \tag{19}$$

where κ_{UAV} is the effective capacitance factor of the UAV.

In this study, the flight energy consumption of the UAV is also considered. The flight energy consumption of a fixed-wing UAV deployed in the discussed system at time slot i can be modelled as [21]

$$E^{\text{fly}}_{\mathrm{U},i} = \delta_i \left(\tau_1 \nu_i^3 + \frac{\tau_2}{\nu_i}\right), \tag{20}$$

where τ_1 and τ_2 are the two parameters related to the weight, wing area, wing span efficiency, and air density of the UAV, respectively.

Therefore, the energy consumption of the UAV at time slot i can be expressed as:

$$E_{\mathrm{U},i} = \mu E^{\text{fly}}_{\mathrm{U},i} + E^{\text{com}}_{\mathrm{U},i}. \tag{21}$$

where μ is the weight of the UAV energy consumption. In this study, the total energy consumption of the UAV consists of two parts: flight energy consumption and computational energy consumption. The weight μ of the flight energy consumption is used to regulate the relative contribution of the two, reflecting the balance between the flight process and computational task energy consumption. The size of the weight μ can be adjusted according to the specific application requirements to optimize energy usage and system performance.

2.3.3. D2D-SeDs Calculate Energy Consumption

Similarly, for the D2D-SeDs offloading part, the SeDs are responsible for providing computational services to the UDs; therefore, the computational energy consumption of the SeDs in time slot i is

$$E_{\mathrm{SeD},i}^{\mathrm{com}} = \sum_{m=1}^{M} \frac{\kappa_m (1 - x_m) \left(\alpha_m L_m\right)^3}{\delta_i^2}. \tag{22}$$

2.4. Problem Formulation

This study aims to maximize the energy efficiency of an IRS-based UAV-D2D collaborative MEC task offload system. Energy efficiency (EE) is defined as the ratio of the total computational tasks in bits to the total energy consumption of the system. The main objective of this section is to maximize the energy efficiency of the MEC system by jointly optimizing the offloading mode selection, UAV trajectory planning, task offloading ratio, MEC computational resource allocation, and IRS phase beamforming. In each time slot, the total energy consumption includes the energy consumption of all UDs, the energy consumption of UAVs, and the energy consumption of the service equipment. The total energy consumption of time slot i is.

$$E_i = E_{m,i} + E_{\mathrm{U},i} + E_{\mathrm{SeD},i}^{\mathrm{com}}. \tag{23}$$

Therefore, the problem of maximizing the energy efficiency of an IRS-based UAV-D2D collaborative MEC mission offloading system can be formulated as follows:

$$\mathcal{P}1: \max_{\{\mathbf{x},\mathbf{z},\boldsymbol{\alpha},\mathbf{f},\boldsymbol{\Theta}\}} \frac{\sum_{i=1}^{I}\sum_{m=1}^{M} L_m}{\sum_{i=1}^{I} E_i} \tag{24a}$$

$$\text{s.t.} \quad x_m \in \{0,1\},\ \forall m \in \mathcal{M}, \tag{24b}$$

$$z_0^{\mathrm{U}} = z_0,\ z_I^{\mathrm{U}} = z_{\mathrm{E}}, \tag{24c}$$

$$0 < \alpha_m < 1,\ \forall m \in \mathcal{M}, \tag{24d}$$

$$\sum_{m=1}^{M} \frac{x_m \alpha_m L_m C_m}{\delta_i} \le F^{\mathrm{U}},\ \forall i \in \mathcal{I}, \tag{24e}$$

$$\frac{(1-\alpha_m) L_m C_m}{\delta_i} \le f_m,\ \forall m \in \mathcal{M},\ i \in \mathcal{I}, \tag{24f}$$

$$\frac{\alpha_m L_m C_m}{\delta_i} \le f_{mk},\ \forall m \in \mathcal{M},\ i \in \mathcal{I}, \tag{24g}$$

$$R_{m,i}^{U} \delta_i \ge \alpha_m L_m,\ \forall m \in \mathcal{M},\ i \in \mathcal{I}, \tag{24h}$$

$$0 \le \theta_n^{(l)} \le 2\pi,\ \forall n \in \{1,2,\ldots,N\}, \tag{24i}$$

$$V_{\min} \le \nu_j \le V_{\max},\ \forall j \in J. \tag{24j}$$

Specifically, constraint (24b) specifies that for any UDs, only one task offload mode can be selected in each time slot, i.e., only one of the tasks can be selected to be offloaded to either the UAVs or the SeDs; (24c) restricts the initial location z_0 and the final location z_E of the UAVs; (24d) is a range of values of offload ratios, which ensures that the remote processing portion of the offloading through the edge servers or the D2D links offloading to SeDs has a positive offloading ratio and does not exceed 1; constraints (24e) and (24f) imply that the workloads of the UAV and UD_m cannot exceed their maximum CPU frequencies; constraint (24g) implies that the workloads of the SeDs cannot exceed their maximum CPU frequencies; (24h) ensures that UD_m is able to offload its tasks to the UAV; and (24i) denotes the phase beam of the lth IRS forming constraints, and (24j) establishes the minimum and maximum flight speeds that limit the UAV.

3. ALGORITHM DESIGN AND IMPLEMENTATION

Owing to the fractional structure of the objective function and the tightly coupled optimization variables in Equation (24), it is difficult to obtain a globally optimal solution. To address these challenges, an iterative algorithm with a two-loop structure was proposed to maximize energy efficiency and optimize offloading mode selection, UAV trajectory planning, mission offloading ratio, MEC computational resource allocation, and IRS phase beamforming [22]. In the outer loop, the Dinkelbach method was used to process the fractional programming and obtain energy efficiency. For a given energy efficiency, the BCD method is used in the inner loop to optimize the coupled variables iteratively. Based on the BCD approach, problem decomposition is combined with an iterative optimization method, which effectively decomposes the complexity into manageable components that are iteratively optimized to obtain a globally optimized solution.

We equivalently transform problem P1 into problem P2:

$$P2: \max_{\{\mathbf{x},\mathbf{z},\boldsymbol{\alpha},\mathbf{f},\boldsymbol{\Theta},\beta\}} \sum_{i=1}^{I}\sum_{m=1}^{M} L_m - \beta \sum_{i=1}^{I} E_i, \tag{25}$$

$$s.t., \quad \text{(24a)–(24k)},$$

where β is the introduced auxiliary parameter. Let β^* denote the maximum energy efficiency achievable for problem P1, and the following theorem holds.

Theorem: The optimal solutions $\{\mathbf{x}^*, \mathbf{z}^*, \boldsymbol{\alpha}^*, \mathbf{f}^*, \boldsymbol{\Theta}^*\}$ of problem (24) are obtained if and only if the following conditions are met:

$$\max_{\{\mathbf{x},\mathbf{z},\boldsymbol{\alpha},\mathbf{f},\boldsymbol{\Phi}\}} \left(\sum_{i=1}^{I}\sum_{m=1}^{M} L_m - \beta^* \sum_{i=1}^{I} E_i \right) = 0. \tag{26}$$

Proof: Prove the theorem under sufficient and necessary conditions. On one hand, according to (26),

$$\left[\sum_{i=1}^{I}\sum_{m=1}^{M} L_m\left(\mathbf{x}^*,\mathbf{z}^*,\boldsymbol{\alpha}^*,\mathbf{f}^*,\boldsymbol{\Theta}^*\right) -\beta^*\sum_{i=1}^{I} E_i\left(\mathbf{x}^*,\mathbf{z}^*,\boldsymbol{\alpha}^*,\mathbf{f}^*,\boldsymbol{\Theta}^*\right)\right]=0$$

And for any other $\{\mathbf{x},\mathbf{z},\boldsymbol{\alpha},\mathbf{f},\boldsymbol{\Theta}\}$,

$$\left[\sum_{i=1}^{I}\sum_{m=1}^{M} L_m\left(\mathbf{x},\mathbf{z},\boldsymbol{\alpha},\mathbf{f},\boldsymbol{\Theta}\right)-\beta^*\sum_{i=1}^{I} E_i\left(\mathbf{x},\mathbf{z},\boldsymbol{\alpha},\mathbf{f},\boldsymbol{\Theta}\right)\right]<0.$$

Therefore, $\frac{\sum_{i=1}^{I}\sum_{m=1}^{M} L_m\left(\mathbf{x}^*,\mathbf{z}^*,\boldsymbol{\alpha}^*,\mathbf{f}^*,\boldsymbol{\Theta}^*\right)}{\sum_{i=1}^{I} E_i\left(\mathbf{x}^*,\mathbf{z}^*,\boldsymbol{\alpha}^*,\mathbf{f}^*,\boldsymbol{\Theta}^*\right)} > \frac{\sum_{i=1}^{I}\sum_{m=1}^{M} L_m\left(\mathbf{x},\mathbf{z},\boldsymbol{\alpha},\mathbf{f},\boldsymbol{\Theta}\right)}{\sum_{i=1}^{I} E_i\left(\mathbf{x},\mathbf{z},\boldsymbol{\alpha},\mathbf{f},\boldsymbol{\Theta}\right)}$ and $\{\mathbf{x}^*,\mathbf{z}^*,\boldsymbol{\alpha}^*,\mathbf{f}^*,\boldsymbol{\Theta}^*\}$ is the optimal solution to the energy efficiency maximization problem (24).

On the other hand, if $\{\mathbf{x}^*,\mathbf{z}^*,\boldsymbol{\alpha}^*,\mathbf{f}^*,\boldsymbol{\Theta}^*\}$ is the optimal solution of (24), then

$$\max_{\{\mathbf{x}^*,\mathbf{z}^*,\boldsymbol{\alpha}^*,\mathbf{f}^*,\boldsymbol{\Theta}^*\}} \frac{\sum_{i=1}^{I}\sum_{m=1}^{M} L_m}{\sum_{i=1}^{I} E_i}=\beta^* \tag{27}$$

Then, after a simple transformation, Equation (26) follows from (27). The existence of a solution set $\{\mathbf{x}^*,\mathbf{z}^*,\boldsymbol{\alpha}^*,\mathbf{f}^*,\boldsymbol{\Theta}^*\}$ that satisfies the equality implies that β^* is the optimal energy efficiency value for problem P1. The theorem is proved.

However, the optimal β^* value is not available in advance. Therefore, we propose an iterative algorithm based on Dinkelbach's method to update β. The details can be found in Algorithm 1.

Algorithm 1 Dinkelbach's algorithm for maximizing energy efficiency

1: initializes $\{\mathbf{x},\mathbf{z},\boldsymbol{\alpha},\mathbf{f},\boldsymbol{\Theta}\}$, iterative number $t=1$, $\delta=10^{-4}$
2: **repeat**
3: solving problem (24) using Algorithm 4 for given a $\beta^{(t)}$, and obtain the optimal solution $\{\mathbf{x}^{(t)},\mathbf{z}^{(t)},\boldsymbol{\alpha}^{(t)},\mathbf{f}^{(t)},\boldsymbol{\Theta}^{(t)}\}$.
4: Calculate$F(\beta^{(t)})=\left|\sum_{i=1}^{I}\sum_{m=1}^{M} L_m-\beta\sum_{i=1}^{I} E_i\right|^{(t)}$
5: **if** $|F(\beta^{(t)})|\le\delta$ **then**
6: $\beta^*=\frac{\sum_{l=1}^{L}\sum_{m=1}^{M} L_m^{(t)}}{\sum_{i=1}^{I} E_i^{(t)}}$,
7: $\{\mathbf{x}^*,\mathbf{z}^*,\boldsymbol{\alpha}^*,\mathbf{f}^*,\boldsymbol{\Phi}^*\}$ $\{\mathbf{x}^{(t)},\mathbf{z}^{(t)},\boldsymbol{\alpha}^{(t)},\mathbf{f}^{(t)},\boldsymbol{\Theta}^{(t)}\}$; **break**;
8: **else**
9: $\beta^{(t+1)}=\frac{\sum_{l=1}^{L}\sum_{m=1}^{M} L_m^{(t)}}{\sum_{i=1}^{I} E_i^{(t)}}$;
10: $t=t+1$;
11: **end if**
12: **Until** $t\ge N_{\max}$
13: **Output:** the optimal energy efficiency β^* and the corresponding solution $\{\mathbf{x}^*,\mathbf{z}^*,\boldsymbol{\alpha}^*,\mathbf{f}^*,\boldsymbol{\Theta}^*\}$.

In Algorithm 1, the outer loop is used to update β, whereas the inner loop is used to solve Problem P2 given $\beta^{(t)}$. However, Problem P2 is still non-convex because of the coupling between the UAV trajectory $\mathbf{z}$, IRS phase $\theta_n^{(l)}$, and other optimization variables for the given energy efficiency C. The outer loop is used to update A, while the inner loop is used to solve Problem P2 given B. However, the outer loop is used to solve Problem P2 given B. Therefore, for Problem P2, the BCD technique is used to decompose it into three subproblems, which are unloading decision and task allocation optimization, trajectory planning and computational resource allocation optimization, and IRS phase optimization. Subsequently, an iterative algorithm for alternating solutions was proposed.

3.1. Offloading Decisions and Task Allocation Optimization

Given $\beta^{(t)}$, a subproblem of P2 is the offloading decision and task allocation optimization, where the UAV trajectory $\mathbf{z}$, MEC computational resource allocation $\mathbf{f}$, and IRS phase $\boldsymbol{\Theta}$ are fixed. Therefore, the offloading decision and task allocation optimization problem can be reformulated according to P2 as

$$\max_{\mathbf{x},\mathbf{a}} \sum_{i=1}^{I}\sum_{m=1}^{M} L_m-\beta\sum_{i=1}^{I} E_i, \tag{28}$$
$$s.t. \quad \text{(24a),(24c)–(24g),}$$

In the task offloading optimization process, two interrelated optimization variables are involved: task offloading mode decision x_m and task offloading ratio α_m, where x_m is a discrete variable that determines whether a task is offloaded to the UAV for computation, and α_m is a continuous variable that indicates the proportion of tasks that are offloaded to the remote device. Because the two are coupled in the optimization process, direct joint optimization will lead to a high complexity of the problem solution. Therefore, to improve the computational efficiency for this sub-problem, alternating optimization is used in the iterations to gradually approach the optimal solution.

Optimize the task offloading ratio α_m given task offloading mode x_m. At this point, the optimization objective can be expressed as

$$\max_{\boldsymbol{\alpha}} \sum_{i=1}^{I}\sum_{m=1}^{M} L_m-\beta\sum_{i=1}^{I} E_i, \tag{29}$$

where the total energy consumption of time slot i is $E_i = E_{m,i}+E_{\mathrm{U},i}+E_{\mathrm{SeD},i}^{\mathrm{com}}$ as shown in Equation (23), and the computed energy consumption of the SeDs was $E_{\mathrm{SeD},i}^{\mathrm{com}}=\sum_{m=1}^{M}\frac{\kappa_m(\alpha_m L_m)^3}{\delta_i^2}$ as shown in Equation (22), and after expanding Equations (18) and (21), respectively.

$$E_{m,i}=\sum_{m=1}^{M}\left(E_{m,i}^{\mathrm{com}}+E_{m,i}^{\mathrm{off}}\right)$$
$$=\sum_{m=1}^{M}\left[\frac{\kappa_m\left[(1-\alpha_m)L_m\right]^3}{\delta_i^2}\right.$$

$$+p_{m,i}\left(x_m\frac{\alpha_m L_m}{R^U_{m,i}}+(1-x_m)\frac{\alpha_m L_m}{R^D_{m,i}}\right)\Bigg] \quad (30)$$

$$E_{\mathrm{U},i}=\mu E^{\mathrm{fly}}_{\mathrm{U},i}+E^{\mathrm{con}}_{\mathrm{U},i}=\mu\delta_i\left(\tau_1\nu_i^3+\frac{\tau_2}{\nu_i}\right)$$

$$+\sum_{m=1}^{M}\frac{\kappa_{\mathrm{UAV}}\left(\alpha_m L_m\right)^3}{\delta_i^2}. \quad (31)$$

For time slot i, the total energy consumption E_i is derived with respect to α_m:

$$\frac{\partial}{\partial\alpha_m}\left(\sum_{i=1}^{I}\sum_{m=1}^{M}L_m-\beta\sum_{i=1}^{I}E_i\right)=0. \quad (32)$$

Substituting the optimization condition from Equation(32) into each energy consumption model:

$$-\beta\sum_{i=1}^{I}\Bigg[\frac{-3\kappa_m(1-\alpha_m)^2L_m^3}{\delta_i^2}$$

$$+p_{m,i}\left(x_m\frac{L_m}{R^U_{m,i}}+(1-x_m)\frac{L_m}{R^D_{m,i}}\right)$$

$$+\frac{3\kappa_{\mathrm{UAV}}\alpha_m^2L_m^3}{\delta_i^2}+\frac{3\kappa_m\alpha_m^2L_m^3}{\delta_i^2}\Bigg]=0 \quad (33)$$

Solve for the optimal task offloading ratio:

$$\alpha_m^*=\frac{1}{\sqrt{\beta\sum_{i=1}^{I}\frac{3L_m^3(\kappa_m+\kappa_{\mathrm{UAV}})}{\delta_i^2}}+1}+\frac{\beta\sum_{i=1}^{I}p_{m,i}\left[\frac{x_m}{R^U_{m,i}}+\frac{1-x_m}{R^D_{m,i}}\right]L_m}{3\beta\sum_{i=1}^{I}\kappa_m L_m^3/\delta_i^2} \quad (34)$$

Ultimately, the solution must be corrected for constraints to ensure that α_m is within the valid range.

$$\alpha_m=\max(0,\min(1,\alpha_m^*)). \quad (35)$$

Optimize the task offloading mode x_m given the task offloading ratio α_m. First, we calculate the computational energy efficiency in the UAV and D2D modes, respectively:

$$EE_U=\frac{\sum_{i=1}^{I}\sum_{m=1}^{M}L_m}{\sum_{i=1}^{I}(E_{m,i}+E_{\mathrm{U},i})},$$

$$EE_D=\frac{\sum_{i=1}^{I}\sum_{m=1}^{M}L_m}{\sum_{i=1}^{I}\left(E_{m,i}+E^{\mathrm{com}}_{\mathrm{SeD},i}\right)}. \quad (36)$$

If the UAV offload mode is more energy efficient, i.e., $EE_U > EE_D$, then select UAV for task offload, at this point, $x_m = 1$. Otherwise, the D2D offload mode was selected: $x_m = 0$.

Algorithm 2 Joint Optimization algorithm for offloading mode and task allocation

Require $L_m, C_m, \delta_i, p_{m,i}, \tau_1, \tau_2, \beta, \mathbf{z}, \mathbf{f}, \mathbf{\Theta}^{(t)}$;
Initialization: Set $t = 0$, maximum iteration $N_{\max}$, and tolerance ϵ
repeat
Step 1: Fix $\mathbf{x}_m$, optimize α_m
for each user m **do**
  Compute α_m^* and project it to feasible region: $\alpha_m = \max(0, \min(1, \alpha_m^*))$
end for
Step 2: Fix α_m, optimize x_m
for each user m **do**
  Compute energy efficiency EE_U, EE_D and choose the better mode: $x_m = \arg\max_{x_m} EE$
end for
Compute the objective value $F^{(t)}$ and check for convergence:
if $|F^{(t)} - F^{(t-1)}| < \epsilon$ **then**
  Converged
end if
Update iteration $t = t + 1$
Until $t \geq N_{\max}$
Ensure Optimal offloading mode $\mathbf{x}^*$ and task proportion $\boldsymbol{\alpha}^*$

3.2. Optimisation of Trajectory Planning and Computational Resource Allocation

In optimization problem P2, UAV trajectory planning and computational resource allocation jointly affected the performance of task offloading, involving UAV flight energy consumption, computational resource scheduling, and wireless link quality. To reduce the energy consumption and improve the task computation efficiency, an alternating optimization approach is used to solve AV trajectory planning and computational resource allocation. Among them, the offloading mode, task offloading ratio, and IRS phase were fixed. Therefore, the trajectory planning and computational resource allocation optimization problem can be reformulated according to P2 as

$$\max_{\mathbf{z},\mathbf{f}}\sum_{i=1}^{I}\sum_{m=1}^{M}L_m-\beta\sum_{i=1}^{I}E_i,$$
$$s.t., \quad (24\mathrm{b}), (24\mathrm{d})\text{–}(24\mathrm{g}), \quad (37)$$

In the case of a fixed UAV flight trajectory $\mathbf{z}$, the optimization problem of computational resource allocation $\mathbf{f}$ focuses on the computational load allocation of the MEC server to maximize the mission computational efficiency and minimize the energy consumption. The reasonable allocation of computational resources can directly affect the mission completion time and overall system energy efficiency; therefore, it is necessary to optimize the UAV computational resources f_m^U. The computational resource allocation of the UAV-MEC server must sat-

isfy the following optimization objectives:

$$\min_{\mathbf{f}} \sum_{i=1}^{I} \left[\mu E_{\mathrm{U},i}^{\mathbf{fly}} + \sum_{m=1}^{M} \frac{\kappa_{UAV} \left(\alpha_m L_m\right)^3}{\left(\delta_i\right)^2} \right] \tag{38}$$

Computational resource allocation satisfies the maximum computational capacity constraint of the UAV server.

$$\sum_{m=1}^{M} \frac{x_m \alpha_m L_m C_m}{\delta_i} \leq F^{\mathrm{U}}, \quad \forall i \in \mathcal{I}. \tag{39}$$

The Lagrangian function for optimizing UAV computational resource allocation is reformulated as follows:

$$\begin{aligned} \mathcal{L}(f_m^U, \lambda_i) \ = \ & \sum_{i=1}^{I} \left[\mu E_{\mathrm{U},i}^{\mathrm{fly}} + \sum_{m=1}^{M} \frac{\kappa_{UAV} \left(\alpha_m L_m\right)^3}{\delta_i^2} \right] \\ & + \sum_{i=1}^{I} \lambda_i \left(\sum_{m=1}^{M} \frac{\alpha_m L_m C_m}{\delta_i} - F^U \right) \end{aligned} \tag{40}$$

where λ_i denotes the Lagrange multiplier.

Next, the first-order necessary conditions for the optimal solution can be obtained by separately taking the derivatives of the UAV computational resource allocation variable f_m^U and making the derivatives zero. By derivation, the closed form of the optimal computational resource allocation solution can be obtained as follows:

$$f_m^{U^*} = \sqrt{\frac{\alpha_m L_m C_m}{\delta_i} \cdot \frac{\beta}{3\kappa_{\mathrm{UAV}}}}, \tag{41}$$

To ensure the effectiveness of the computational resource allocation, it is also necessary to correct the constraints of the obtained optimal solution such that it meets the actual constraints of the UAV computational resources:

$$f_m^U = \min \left(F^U, f_m^{U^*} \right). \tag{42}$$

With a fixed computational resource allocation $\mathbf{f}$, the planning of the UAV flight trajectory $\mathbf{z}$ has a crucial impact on the computational offloading efficiency and total energy consumption of the system. Owing to the high degrees of freedom of motion of the UAV, trajectory planning involves multiple decision variables, making the problem non-convex. To ensure the lowest energy consumption flight under the UAV computational capacity constraints, a gradient descent-based optimization method is used to update the UAV trajectory step-by-step to minimize the total energy consumption of the system. The planning of the UAV flight trajectory must satisfy the following optimization objectives:

$$\min_{\mathbf{z}} \sum_{i=1}^{I} \left[\mu E_{\mathcal{U},i}^{\mathrm{fly}} + \sum_{m=1}^{M} \frac{\kappa_{UAV} (\alpha_m L_m)^3}{\delta_i^2} \right] \tag{43}$$

At this point, the flight energy consumption of the UAV at the ith time slot can be explicitly expressed as:

$$E_{\mathrm{U},i}^{\mathrm{fly}} = \delta_i \left(\tau_1 \|\mathbf{v}_i\|^3 + \frac{\tau_2}{\|\mathbf{v}_i\|} \right) \tag{44}$$

where $\mathbf{v}_i$ denotes the flight speed of the UAV at time slot i, which is defined as $\mathbf{v}_i = \frac{\mathbf{z}_i^{\mathrm{U}} - \mathbf{z}_{i-1}^{\mathrm{U}}}{\delta_i}$.

To ensure that the UAV's flight trajectory meets the system's practical requirements, the specific constraints are as follows: UAV trajectory planning must satisfy positional constraints $z_0^{\mathrm{U}} = z_0$, $z_I^{\mathrm{U}} = z_{\mathrm{E}}$ and velocity constraints $V_{\min} \leq \nu_j \leq V_{\max}$, $\forall j \in J$. Although the velocity constraint itself is convex, when coupled with the UAV flight energy consumption expression (44), the entire trajectory planning subproblem exhibits non-convexity.

To solve the above non-convex optimization problem, this study uses an iterative optimization algorithm based on the gradient descent method to update the trajectory. Specifically, we first provide the gradient expression for the flight energy consumption with respect to velocity $\mathbf{v}_i$:

$$\frac{\partial E_{\mathrm{U},i}^{\mathrm{fly}}}{\partial \mathbf{v}_i} = 3\mu\tau_1\delta_i \|\mathbf{v}_i\| \mathbf{v}_i - \mu\tau_1\delta_i \frac{\mathbf{v}_i}{\|\mathbf{v}_i\|^3} \tag{45}$$

Then, based on the relationship between velocity and UAV trajectory position:

$$\frac{\partial \mathbf{v}_i}{\partial \mathbf{z}_i} = \frac{\mathbf{z}_i^U - \mathbf{z}_{i-1}^U}{\delta_i \|\mathbf{z}_i^U - \mathbf{z}_{i-1}^U\|} \tag{46}$$

Thus, the gradient expression for the UAV trajectory position $\mathbf{z}_i$ is explicitly stated as:

$$\nabla_{\mathbf{z}_i} \left(\mu E_{\mathrm{U},i}^{\mathbf{fy}} \right) = \mu \left(3\tau_1 \| \mathbf{v}_i \|^2 + \frac{\tau_1}{\| \mathbf{v}_i \|^3} \right) \frac{\mathbf{z}_i^U - \mathbf{z}_{i-1}^U}{\| \mathbf{z}_i^U - \mathbf{z}_{i-1}^U \|} \tag{47}$$

Based on the gradient descent method, the update rules for the UAV trajectories are as follows:

$$\mathbf{z}_i^{(t+1)} = \mathbf{z}_i^{(t)} - \gamma \nabla_{\mathbf{z}_i^U} \left(\mu E_{\mathrm{U},i}^{\mathrm{fly}} \right). \tag{48}$$

where $\gamma > 0$ is the step factor of the algorithm.

3.3. IRS Phase Shift Optimization

Consider that another subproblem of problem P2 is IRS phase-shift optimization, where the task offloading mode decision, UAV trajectory, task offloading ratio, and MEC computational resource allocation are fixed. Therefore, the IRS phase-shift optimization problem can be reformulated according to P2 as

$$\begin{aligned} & \max_{\mathbf{\Theta}} \sum_{i=1}^{I} \sum_{m=1}^{M} L_m - \beta \sum_{i=1}^{I} E_i, \\ & s.t., \quad (24\mathrm{h}). \end{aligned} \tag{49}$$

Algorithm 3 Joint optimization algorithm for UAV trajectories and computational resources

Require $\mathbf{x}, \boldsymbol{\alpha}, \boldsymbol{\Theta}^{(t)}, \delta_i, \alpha_m, \tau_1, \tau_2, F^U, \nu_{\min}, \nu_{\max}$;
Initialization: $\mathbf{z}$, $\mathbf{z}$, maximum iteration $N_{\max}$, Step size η, tolerance ϵ and Iteration count $t = 0$;
repeat
Step 1: Fix z, optimize f;
Fixed UAV trajectories optimize computational resources according to computational resource constraints **f**: $f_m^U = \min(F^U, f_m^{U^*})$;
Step 2: Fix f, optimize z
for Each time slot i **do**
  Calculate the flight energy consumption of the UAV at time slot i: $E_{\mathrm{U},i}^{\mathrm{fly}} = \delta_i \left(\boldsymbol{\tau}_1 \|\mathbf{v}_i\|^3 + \frac{\boldsymbol{\tau}_2}{\|\mathbf{v}_i\|}\right)$;
  Updating of UAV tracks $\mathbf{z}: \mathbf{z}_i^{(t+1)} = \mathbf{z}_i^{(t)} - \gamma \nabla_{\mathbf{z}_i^U} \left(\boldsymbol{\mu} E_{\mathrm{U},i}^{\mathrm{fly}}\right)$;
  Ensure that the UAV trajectory satisfies the velocity constraints: $\nu_{\min} \le \nu_i \le \nu_{\max}$;
end for
Step 3: Convergence judgements;
compute the objective value $F^{(t)}$ and check for convergence:
if $\mid \mathbf{z}_i^{(t+1)} - \mathbf{z}_i^{(t)} \mid < \epsilon$ **then**
  End of iteration:
end if
Update iteration $t = t + 1$
Until $t \ge N_{\max}$
Ensure Optimal UAV trajectory $\mathbf{z}^*$ and Computation resource allocation $\boldsymbol{\alpha}^*$

Because all other variables are fixed at this stage, a part of the above optimization problem that is directly related to the IRS phase shift matrix $\boldsymbol{\Theta}$ is the channel gain of the communication link, expanding Equations (9) and (11) to obtain Algorithm 3.

If the offload mode of UD_m is the UAV mode ($x_m = 1$), the effective communication rate can be expressed as:

$$R_{m,i}^U(\Theta) = B^U \log_2\left(1 + \frac{p_{m,i}\left|h_{m,U} + (\mathbf{h}_{m,R})^H \boldsymbol{\Theta}^{(l)} \mathbf{h}_{R,U}\right|^2}{\sigma^2}\right) \tag{50}$$

If the offload mode of UD_m is the D2D mode ($x_m = 0$), the effective communication rate can be expressed as:

$$R_{m,i}^D(\Theta) = B^D \log_2\left(1 + \frac{p_{m,i}\left|h_{m,k} + (\mathbf{G}_{d2d})^H \boldsymbol{\Theta}^{(l)} \mathbf{h}_{m,k}^R\right|^2}{\sigma_{d2d}^2}\right) \tag{51}$$

Therefore, the IRS phase shift optimization problem is:

$$\max_{\boldsymbol{\Theta}} \sum_{i=1}^{I} \sum_{m=1}^{M} \left[x_m R_{m,i}^U(\boldsymbol{\Theta}) + (1 - x_m) R_{m,i}^D(\boldsymbol{\Theta})\right] \tag{52}$$

Each reflective unit within the IRS must satisfy the unit modulus length constraint $|\Theta_{n,n}| = 1$. The set of these constraints forms a complex circular manifold with nonconvex properties, making it difficult to solve directly. Therefore, iterative optimization was performed using the successive convex approximation (SCA) method. At the tth iteration, the objective function is approximated by a first-order Taylor expansion at the previous iteration phase-shift matrix $\boldsymbol{\Theta}^{(t)}$. The objective function is then approximated by a first-order Taylor expansion at the tth iteration:

$$f(\boldsymbol{\Theta}) \approx f(\boldsymbol{\Theta}^{(t)}) + \mathrm{Re}\left\{\mathrm{tr}\left[(\nabla_{\boldsymbol{\Theta}} f(\boldsymbol{\Theta}^{(t)}))^H (\boldsymbol{\Theta} - \boldsymbol{\Theta}^{(t)})\right]\right\} \tag{53}$$

where the gradient of the objective function is expressed as:

$$\begin{aligned}
&\nabla_{\boldsymbol{\Theta}} f(\boldsymbol{\Theta}^{(l)}) \\
&= \sum_{i=1}^{I} \sum_{m=1}^{M} \frac{2 p_{m,i} x_m \mathbf{h}_{m,R} (\mathbf{h}_{R,U})^H \left[h_{m,U} + (\mathbf{h}_{m,R})^H \boldsymbol{\Theta}^{(l)} \mathbf{h}_{R,U}\right]}{\sigma^2 \ln 2 \left[1 + \frac{p_{m,i}\left|h_{m,U} + (\mathbf{h}_{m,R})^H \boldsymbol{\Theta}^{(l)} \mathbf{h}_{R,U}\right|^2}{\sigma^2}\right]} \\
&+ \frac{2 p_{m,i} (1 - x_m) \mathbf{G}_{d2d} (\mathbf{h}_{m,k}^R)^H \left[h_{m,k} + (\mathbf{G}_{d2d})^H \boldsymbol{\Theta}^{(l)} \mathbf{h}_{m,k}^R\right]}{\sigma_{d2d}^2 \ln 2 \left[1 + \frac{p_{m,i}\left|h_{m,k} + (\mathbf{G}_{d2d})^H \boldsymbol{\Theta}^{(l)} \mathbf{h}_{m,k}^R\right|^2}{\sigma_{d2d}^2}\right]}.
\end{aligned} \tag{54}$$

Using the gradient expression above, the IRS phase-shift matrix is updated using Equation (50).

$$\boldsymbol{\Theta}^{(t+1)} = \exp\left\{j \cdot \arg\left[\boldsymbol{\Theta}^{(t)} + \eta \nabla_{\boldsymbol{\Theta}} f(\boldsymbol{\Theta}^{(t)})\right]\right\} \tag{55}$$

where $\eta > 0$ denotes the step factor of the gradient update. After each update, the IRS phase shift matrix must satisfy the phase constraint.

The above iterative process is repeated until the following convergence conditions are satisfied:

$$\left|f(\Theta^{(t+1)}) - f(\Theta^{(t)})\right| < \epsilon \tag{56}$$

where $\epsilon > 0$ is a predetermined convergence threshold.

Based on the above method, a new phase shift matrix is obtained in each iteration by maximizing this approximate function. Since the approximate function serves as an upper bound of the original function, with $f(\Theta^{(t+1)}; \Theta^{(t)}) \ge f(\Theta^{(t)}; \Theta^{(t)}) = f(\Theta^{(t)})$, the value of the original function at the new point is guaranteed to be no less than that at the current point. Therefore, the objective function value is non-decreasing throughout the iterative process. Meanwhile, because the feasible set of phase shift matrices is compact, the generated sequence must have a convergent subsequence. By incorporating the gradient consistency condition, any limit point can be proved to satisfy the first-order optimality condition, thus being a stationary point.

Based on the obtained solutions of the three subproblems, the BCD algorithm for solving problem (25) with a given energy efficiency is summarized in Algorithm 5. Therefore, the original non-convex problem (24) can be solved efficiently by iteratively updating the energy efficiency in the outer loop according to Algorithm 1 and jointly optimizing the offloading

Algorithm 4 IRS phase shift optimization algorithm based on SCA approach

Require $L_m, C_m, \delta_i, p_{m,i}, \tau_1, \tau_2, \beta, \mathbf{x}, \alpha, \mathbf{z}, \mathbf{f}$;
Initialization: $\boldsymbol{\Theta}^{(t)}$, maximum iteration $N_{\max}$, Step size η, tolerance ϵ and Iteration count $t = 0$;
repeat
Calculate the gradient $\nabla_{\boldsymbol{\Theta}} f(\boldsymbol{\Theta}^{(t)})$ from $\boldsymbol{\Theta}^{(t)}$:
Update the IRS phase shift matrix based on the gradient: $\boldsymbol{\Theta}^{(t+1)} = \exp\left\{j \cdot \arg\left(\boldsymbol{\Theta}^{(t)} + \boldsymbol{\eta}\nabla_{\boldsymbol{\Theta}} f(\boldsymbol{\Theta}^{(t)})\right)\right\}$;
Make constraint corrections: $\mid \Theta_{n,n}^{(t+1)} \mid = 1, \forall n$;
Update iteration $t = t + 1$;
Until $\left|f(\Theta^{(t+1)}) - f(\Theta^{(t)})\right| < \epsilon$;
Ensure Optimal IRS phase shift matrix $\boldsymbol{\Theta}^* = \boldsymbol{\Theta}^{(t+1)}$;

mode selection, UAV trajectory, task offloading ratio, MEC computational resource allocation, and IRS phase-shift in the inner loop through Algorithm 5.

Algorithm 5 BCD-based energy efficiency optimization algorithm for IRS-assisted UAV-D2D collaborative MEC system

Require $\mathcal{X}_m^{(0)}, \boldsymbol{\alpha}_m^{(0)}, \mathbf{z}_i^{U,(0)}, f_m^{U,(0)}, \boldsymbol{\Theta}^{(0)}, \epsilon, T_{\max}$;
Initialization: Iteration count $t = 0$;
repeat
Given $\mathbf{z}_i^{U,(t)}$, $f_m^{U,(t)}$, and $\boldsymbol{\Theta}^{(t)}$, call Algorithm 2 to update: $\{x_m^{(t+1)}\}$, $\{\alpha_m^{(t+1)}\}$:
Given the updated $\{x_m^{(t+1)}\}$, $\{\alpha_m^{(t+1)}\}$, $\boldsymbol{\Theta}^{(t)}$, call Algorithm 3 to update: $\{\mathbf{z}_i^{U,(t+1)}\}$, $\{f_m^{U,(t+1)}\}$;
Given the updated $\{x_m^{(t+1)}\}$, $\{\alpha_m^{(t+1)}\}$, $\{\mathbf{z}_i^{U,(t+1)}\}$, $\{f_m^{U,(t+1)}\}$, call Algorithm 4 to update: $\boldsymbol{\Theta}^{(t)}$;
Calculate the current objective function value: $F^{(t+1)} = \sum_{i=1}^{I}\sum_{m=1}^{M} L_m - \beta\sum_{i=1}^{I} E_i$;
Update iteration $t = t + 1$;
Until Satisfying convergence conditions $\left|F^{(t)} - F^{(t-1)}\right| \leq \epsilon$ or $t \geq T_{\max}$;
Ensure Optimal uninstallation mode $\{x_m^*\}$, Mission offloading ratio $\{\alpha_m^*\}$, UAV trajectory $\{\mathbf{z}_i^{U,*}\}$, Computation resource allocation $\{f_m^{U,*}\}$, Optimal IRS phase shift matrix $\boldsymbol{\Theta}^*$;

To analyze the computational complexity of the proposed IRS-D2D-MEC cooperative offloading strategy, the entire optimization process is divided into three modules: offloading mode selection, resource allocation, and IRS phase optimization. The analysis is presented as follows.

Offloading mode selection (potential game): With M user devices, each user considers the strategies of the other $M-1$ users in each round of the game. Therefore, the complexity of a single-round update is $O(M^2)$. Convergence to a Nash equilibrium requires I_1 rounds. Hence, the total complexity for this module is $O(I_1 \cdot M^2)$.

Resource allocation (Lagrange + KKT): With a fixed offloading strategy, bandwidth and computing frequency are jointly allocated. The number of resources is K. The computational complexity per iteration is $O(MK)$.

IRS phase optimization (gradient descent): The number of IRS reflecting elements is N. Optimizing the phase for each element requires calculating the complex channel gain. Each iteration has a complexity of $O(N^2)$. With a total of I_2 iterations, the complexity of this part is $O(I_2 \cdot N^2)$.

Therefore, the total complexity of the overall algorithm is approximately $O(I_1 \cdot M^2 + MK + I_2 \cdot N^2)$. Under conditions where $N \geq M, K$, the main computational overhead lies in the IRS phase control part. Considering that the IRS can be accelerated by parallel processing circuits or approximate linear methods, the overall complexity remains within an acceptable polynomial range.

4. SIMULATION RESULTS AND ANALYSIS

This section presents the results of the IRS-assisted UAV-D2D collaborative MEC offloading to improve energy efficiency, including the properties of the proposed algorithm and energy efficiency performance in a simulated environmental scenario.

In the simulation, a UAV-enabled MEC system is considered with UDs and SeDs dispersed using a Normal Distribution (ND), where the UAV flight altitude is set to 100 m, maximum flight speed $\nu_{\max} = 50$ km/h, minimum flight speed $\nu_{\max} = 3$ km/h, and maximum acceleration $\nu_{\max}^a = 5$ m/s^2. The UAVs were then unloaded into an IRS-assisted MEC system. The horizontal position of the first element on the IRS was $[50, 25]$ m; the height was 20 m; and the number of reflective elements was to $N = 40$. It is assumed that the UDs have the same number of task input bits. Other key parameters are listed in Table 1. In the following, simulation tests of the total system delay are performed for the variables of the UAV trajectory, total number of the task input bits, reflective elements N, and UDs.

TABLE 1. Main parameters of the simulation.

Description	Parameter and Value
Location model	$R = 500$ m, $H = 100$ m
	$v_{\max} = 50$ km/h
Computing model	Number of time slots $I = 20$
	$\tau_1 = 0.00614$, $\tau_2 = 15.976$
	$F_U = 15 \times 10^9$
Communication model	$B^U = 20$ MHZ, $B^D = 10$ MHZ
	$\sigma_M = 10^{-6}$, $\sigma_D = 7 \times 10^{-7}$
Convergence criterion	$\epsilon = 0.001$

To demonstrate the superior performance of the proposed algorithmic system, the performance of the proposed scheme was evaluated by comparing it with the following four benchmark schemes:

(1) No trajectory optimization: the trajectory of the UAV follows a straight line from the initial position to the final position. The offloading mode and task scaling are implemented using Algorithm 2, the computational resource allocation is otherwise still handled by the Lagrange mul-

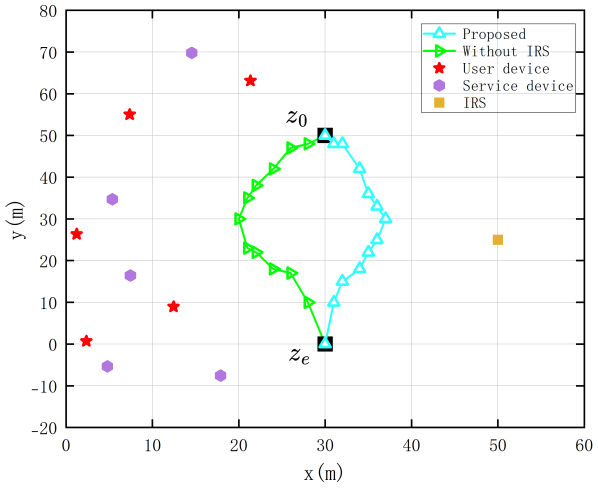

FIGURE 2. UAV flight trajectories for two different scenarios: the algorithm proposed in this section and the IRS-free scheme.

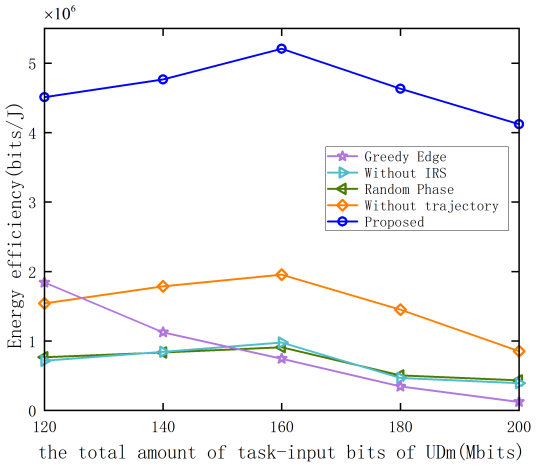

FIGURE 3. Plot of energy efficiency versus total UDs task input bits.

tiplier method, and the IRS phase optimization is implemented using Algorithm 4.

(2) Stochastic phasing: Algorithms 1 and 2 are used to optimize the offloading mode, edge computational resource allocation, and offloading ratio of the UDs. The step of designing the IRS phase is also skipped, and the IRS phase was set randomly, obeying a uniform distribution in the range of $[0, 2\pi)$.

(3) No IRS: The reflection channel of the IRS was set to 0. The offloading mode selection, edge computing resource allocation, and offloading ratio of the UDs are designed according to Algorithms 1 and 2.

(4) Edge greedy: Each UD performs task offloading through the UAV edge server without involving D2D offloading [23].

First, the UAV trajectory for the IRS-based UAV-D2D-assisted MEC system is illustrated. Figure 2 illustrates the flight trajectories of the UAV under two different scenarios: the algorithm proposed in this section and the no-IRS scenario [24]. In the scenario without the IRS, it can be observed that the UAV tends to fly closer to UD to obtain a higher channel gain. In contrast, in the UAV-MEC system with IRS assistance proposed in this study, it is observed that the UAV tends to fly closer to the IRS. This is because the UAV needs to compromise between a direct link and an IRS-reflected link when an IRS is deployed to assist the UD offloading task. By adjusting the phase shift of the IRS using the algorithms presented in this section, the reflected signals can be coherent to significantly increase the received signal power of the UAV. As a result, UAVs tend to fly closer to the IRS rather than the UD to fully utilize the channel gain from the IRS and improve the EE.

The proximity of a UAV to an IRS alters its three-dimensional spatial position. Different flight altitudes cause the channel to exhibit varying fading characteristics. However, with the proposed trajectory planning algorithm, the flight altitude can be adaptively adjusted. A balance is sought between flight energy consumption and communication quality. Furthermore, the IRS phase shifts are optimized based on real-time channel conditions. Whether the channel follows Rayleigh fading or Rician fading, the reflection coefficients are adaptively optimized. Consequently, the impact of UAV flight altitude on channel characteristics does not hinder the system's energy efficiency improvement.

The UDs, SeDs, and IRS reflective elements are set to $M = 10$, $K = 20$ and $N = 40$, respectively. Figure 3 shows the energy efficiency of the system versus the total UDs task input bits, where the energy efficiency maximization algorithm proposed in this section is compared with the other four schemes. It can be seen that after deploying the IRS, the proposed algorithm can achieve higher EE than the other schemes owing to the joint optimization of the offloading mode and task offloading ratio, UAV trajectory and computational resource allocation, and IRS phase. In addition, it can be seen that the EE of the other schemes first increases and then decreases, with the exception of the full UAV offloading scheme. According to [25], the total offloading energy consumption of UD can be expressed as an exponential function related to the offloading data rate. Because the exponential function grows faster than the linear function, EE first increases and then decreases as the offload data rate increases. Therefore, when the total number of task input bits increases, EE first increases and then decreases. For the full UAV offloading scheme, the EE only shows a decreasing trend because the full UAV offloading scheme leads to resource constraints on the UAV edge servers, and the energy consumption is much higher than that of the other schemes. It can also be observed that if random IRS phasing is chosen, the performance gain brought about by random IRS phasing is almost negligible with respect to the no-IRS scheme. This is because in the random phase scheme, when these signals reflected through the IRS are merged at the UAV, the channel gain of the reflected link is almost equal to zero. This result demonstrates the importance of phase optimization in IRS-assisted UAV-D2D collaborative MEC systems.

In the theoretical analysis, the IRS is assumed to have continuous phase shifts. However, in practical hardware, discrete

phase shifts are often present at IRS elements. Although discrete phase shifts introduce some performance loss, the main conclusions remain robust. First, compared to schemes without an IRS, the IRS-assisted UAV-D2D cooperative MEC system still exhibits an advantage in energy efficiency. The introduction of the IRS itself is an effective means of improving energy efficiency. The fundamental conclusion is not altered by discrete phase shifts. Second, the proposed iterative optimization framework demonstrates a certain adaptability to phase quantization. Performance loss caused by quantization can be partially compensated during the optimization process. Moreover, in practical deployment, an appropriate number of quantization bits can be selected based on hardware cost and performance requirements. A balance can be achieved between these two factors. Therefore, discrete phase shifts do not affect the core conclusion: with IRS assistance, the UAV-D2D cooperative MEC system can effectively improve energy efficiency.

The SeDs, IRS reflection elements, and total task input bits were set to $M = 10$, $K = 20$, and 160 (Mbits), respectively. Figure 4 shows the trend of the system EE with the number of UDs for different optimization schemes. It can be observed that the optimization scheme of this study is significantly better than the other comparison schemes, and the EE gradually increases when the UDs are small and slightly decreases after the number of UDs reaches 12, which indicates that the appropriate number of UDs helps in MEC task offloading, while too many devices lead to limited computational resources, which reduces the EE. Under the Without Trajectory Optimization scenario shows that Although the EE is lower than the proposed scenario, it still maintains a high level and increases and then decreases with the number of UDs. This indicates that even without UAV trajectory optimization, proper task offloading and IRS reflection gain can still improve EE; however, the heavy UAV computational load fails to make full use of the optimal flight path to reduce energy consumption. In contrast, the Random Phase and Without IRS schemes have a significantly lower EE, and the EE does not change significantly or even decreases when the number of UDs increases. It indicates that the phase optimization of the IRS reflected signal has a significant impact on the EE, and the failure to optimize the IRS phase prevents the UAV from making full use of the reflected channel gain, which leads to a decrease in the EE. In addition, in the Without IRS scheme, the UAV can only rely on the UDs to directly connect to the channel, and its EE is significantly lower than that of the optimized schemes studied in this section, indicating that the IRS plays a key role in the UAV mission offloading process. The Greedy Edge scheme has the lowest EE, and the EE continues to decrease with the increase in the number of UDs, suggesting that when the UAV is unable to collaborate in the offloading with the aid of D2D. When the tasks all rely on UAV computation, the EE is limited by the computational resources and cannot be scaled effectively. This further validates the necessity of D2D collaborative offloading optimization. This experiment verifies that IRS-assisted D2D offloading and UAV trajectory optimization can effectively improve the EE of task offloading. Moreover, the curve illustrating the impact of UD quantity changes on system energy efficiency indicates the existence of an optimal D2D load range within the system. The results demonstrate that the proposed solution maintains effective performance under D2D load conditions and exhibits excellent scalability. The scheme proposed in this section considers UAV trajectory optimization, IRS phase optimization, and D2D task offloading strategy, and is able to maintain a higher EE under different numbers of users, while the EE of the scheme without IRS, D2D, or UAV trajectory optimization drops significantly. This demonstrates the important role of the IRS in UAV computational offloading and further proves the necessity of UAV trajectory optimization to improve EE.

The UDs and IRS reflective elements, respectively, and the total task input bits were set to $M = 10$, $N = 40$ and 160 (Mbits). Figure 5 demonstrates the effect of different algorithms on the system EE with varying numbers of SeDs. The results show that the energy efficiency of all the algorithms shows an increasing trend with the increase in the number of SeDs, but the performance difference between the algorithms is significant. Among them, the proposed scheme achieves significant energy efficiency gains by jointly optimizing the UAV trajectory, IRS reflection phase, and resource allocation strategy, which outperforms the other compared algorithms under all the conditions of the number of SeDs, verifying its superi-

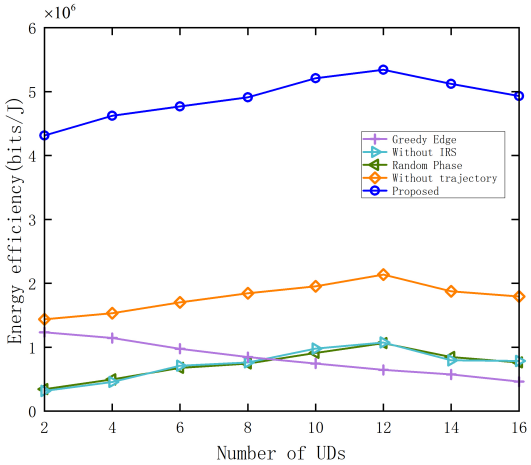

FIGURE 4. Plot of energy efficiency versus number of UDs.

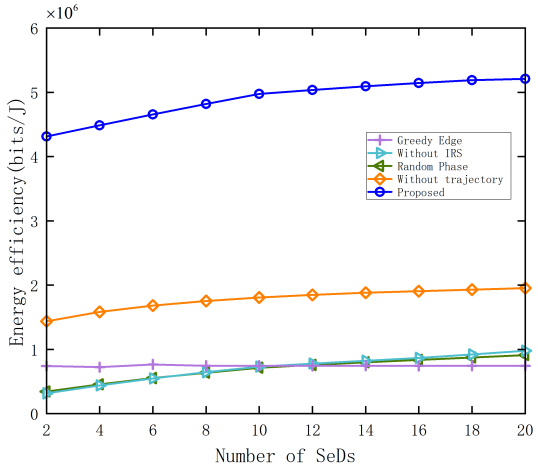

FIGURE 5. Plot of energy efficiency versus number of SeDs.

ority. While the Without trajectory scheme can improve part of the energy efficiency, its performance is still significantly lower than that of the proposed algorithm, indicating that the dynamic adjustment of the UAV trajectory is crucial for energy efficiency optimization. In addition, the IRS algorithms using the Random Phase scheme and Without IRS scheme have similar performance, both of which are significantly better than the Greedy Edge scheme, but much less than the joint optimization scheme, further highlighting the importance of IRS phase optimization. It is particularly noteworthy that the Greedy Edge algorithm does not have SeDs for auxiliary task offloading; thus, changes in the number of SeDs have no effect on the algorithm, again reflecting the difficulty of relying solely on the locally optimal policy to achieve global performance enhancement in complex multi-user environments.

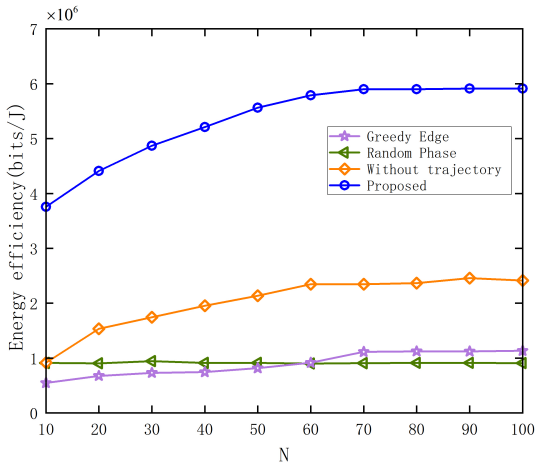

FIGURE 6. Plot of energy efficiency versus number of IRS reflective units (N).

The UDs, SeDs, and total task input bits $M = 10$, $K = 20$ and 160 (Mbits), respectively. As can be seen in Figure 6, the EE of all schemes except the Random Phase scheme increases with the number of IRS elements and starts to level off at the number of reflection elements N equal to 70. This is because additional reflection elements provide additional degrees of freedom for designing more efficient phase-shifting strategies. The algorithm proposed in this study consistently outperformed without Trajectory Optimization, Random Phase scheme, and the Greedy Edge scheme. This is because offloading pattern and task ratio, UAV trajectory and computational resource allocation, and IRS phase shifting are jointly considered in the algorithms proposed in this section. It should be noted that the performance gap between the proposed algorithm and Random Phase scheme increases as the number of IRS elements increases, which further validates that the joint optimization of the offloading mode with task ratio, UAV trajectory with computational resource allocation, and IRS phase-shift superiority are jointly considered. Under varying IRS configurations, practical deployment also necessitates balancing performance gains against hardware costs. It is noted that the performance gap between the proposed algorithm and random phase scheme gets larger as the number of IRS elements increases, which further validates the necessity of jointly optimizing the offloading mode with the task ratio, UAV trajectory with computational resource allocation, and IRS phase-shift optimization.

5. CONCLUSIONS

In this study, IRS-based D2D-assisted MEC collaborative offloading is investigated, with further consideration given to the incorporation of UAV scenarios. A joint optimization strategy for maximizing the energy efficiency is proposed. This study suggests a dual-loop iterative optimization framework that combines the Dinkelbach and BCD algorithms. The framework addresses the challenges of high coupling and nonconvexity by focusing on three major areas: offloading decisions and task allocation, UAV trajectory planning and computational resource allocation, and IRS phase-shift optimization. This approach meets the low-latency, high-energy-efficiency requirements of UDs, advancing the development of collaborative networks, including IRS, D2D communication, MEC, and UAV trajectory planning. Additionally, the proposed algorithm maintains a high energy efficiency under varying task loads and user counts, demonstrating its practical application potential in real-world environments. The joint optimization strategy not only enhances energy efficiency, but also provides a valuable reference for network infrastructure deployment and operational cost considerations. However, with the increasing demand for 6G and advancements in MEC, current research faces several challenges. For instance, the present research primarily focuses on the cooperative optimization of a single UAV and IRS, neglecting the computational complexity or energy consumption associated with large-scale IRS deployments, as well as the robustness of algorithms in dynamic environments. Therefore, these areas warrant further investigation in future research.

ACKNOWLEDGEMENT

This work was supported by the Natural Science Foundation of Fujian Province (Grant No. 2023I0044), Undergraduate Education and Teaching Research Project of Fujian Province (Grant No. FBJY20240120), and High-level Talent Project of Xiamen University of Technology (Grant No. YKJ23034R), and the Postgraduate Science and Technology Innovation Project of the Xiamen University of Technology (Grant No. YKJCX2025139).

REFERENCES

[1] Zhou, J., C. Feng, Y. Sun, and J. Guo, "Minimization of latency in D2D-assisted MEC collaborative offloading based on intelligent reflecting surface," *Progress In Electromagnetics Research B*, Vol. 110, 1–14, 2025.

[2] Wu, Q. and R. Zhang, "Towards smart and reconfigurable environment: Intelligent reflecting surface aided wireless network," *IEEE Communications Magazine*, Vol. 58, No. 1, 106–112, 2020.

[3] Liu, Y., X. Liu, X. Mu, T. Hou, J. Xu, M. D. Renzo, and N. Al-Dhahir, "Reconfigurable intelligent surfaces: Principles and opportunities," *IEEE Communications Surveys & Tutorials*, Vol. 23, No. 3, 1546–1577, 2021.

[4] Truong, P. Q., T. Do-Duy, A. Masaracchia, N.-S. Vo, V.-C. Phan, D.-B. Ha, and T. Q. Duong, "Computation offloading and resource allocation optimization for mobile edge computing-aided UAV-RIS communications," *IEEE Access*, Vol. 12, 107 971–107 983, 2024.

[5] Lu, J., W. Feng, and D. Pu, "Resource allocation and offloading decisions of D2D collaborative uavassisted MEC systems," *KSII Transactions on Internet & Information Systems*, Vol. 18, No. 1, 211–232, 2024.

[6] Li, Y., C. Yin, T. Do-Duy, A. Masaracchia, and T. Q. Duong, "Aerial reconfigurable intelligent surface-enabled URLLC UAV systems," *IEEE Access*, Vol. 9, 140 248–140 257, 2021.

[7] Nguyen, M.-H. T., E. Garcia-Palacios, T. Do-Duy, O. A. Dobre, and T. Q. Duong, "UAV-aided aerial reconfigurable intelligent surface communications with massive MIMO system," *IEEE Transactions on Cognitive Communications and Networking*, Vol. 8, No. 4, 1828–1838, 2022.

[8] Do-Duy, T., D. V. Huynh, E. Garcia-Palacios, T.-V. Cao, V. Sharma, and T. Q. Duong, "Joint computation and communication resource allocation for unmanned aerial vehicle NOMA systems," in *2023 IEEE 28th International Workshop on Computer Aided Modeling and Design of Communication Links and Networks (CAMAD)*, 290–295, Edinburgh, United Kingdom, 2023.

[9] Wang, Y., J. Niu, G. Chen, X. Zhou, Y. Li, and S. Liu, "RIS-aided latency-efficient MEC HetNet with wireless backhaul," *IEEE Transactions on Vehicular Technology*, Vol. 73, No. 6, 8705–8719, 2024.

[10] Xu, Y., T. Zhang, Y. Zou, and Y. Liu, "Reconfigurable intelligence surface aided UAV-MEC systems with NOMA," *IEEE Communications Letters*, Vol. 26, No. 9, 2121–2125, 2022.

[11] Hu, H., Z. Sheng, A. A. Nasir, H. Yu, and Y. Fang, "Computation capacity maximization for UAV and RIS cooperative MEC system with NOMA," *IEEE Communications Letters*, Vol. 28, No. 3, 592–596, 2024.

[12] Hamid, H. and G. R. Begh, "IRS assisted UAV communications for 6G networks: A systematic literature review," *Wireless Networks*, Vol. 31, No. 1, 779–807, 2025.

[13] Jeong, S., O. Simeone, and J. Kang, "Mobile edge computing via a UAV-mounted cloudlet: Optimization of bit allocation and path planning," *IEEE Transactions on Vehicular Technology*, Vol. 67, No. 3, 2049–2063, 2018.

[14] Motlagh, N. H., M. Bagaa, and T. Taleb, "UAV-based IoT platform: A crowd surveillance use case," *IEEE Communications Magazine*, Vol. 55, No. 2, 128–134, 2017.

[15] Ji, J., K. Zhu, C. Yi, and D. Niyato, "Energy consumption minimization in UAV-assisted mobile-edge computing systems: Joint resource allocation and trajectory design," *IEEE Internet of Things Journal*, Vol. 8, No. 10, 8570–8584, 2021.

[16] Mei, H., K. Yang, J. Shen, and Q. Liu, "Joint trajectory-task-cache optimization with phase-shift design of RIS-assisted UAV for MEC," *IEEE Wireless Communications Letters*, Vol. 10, No. 7, 1586–1590, 2021.

[17] Ranjha, A. and G. Kaddoum, "URLLC facilitated by mobile UAV relay and RIS: A joint design of passive beamforming, blocklength, and UAV positioning," *IEEE Internet of Things Journal*, Vol. 8, No. 6, 4618–4627, 2021.

[18] Zhang, X., J. Zhang, J. Xiong, L. Zhou, and J. Wei, "Energy-efficient multi-UAV-enabled multiaccess edge computing incorporating NOMA," *IEEE Internet of Things Journal*, Vol. 7, No. 6, 5613–5627, 2020.

[19] Liu, B., Y. Wan, F. Zhou, Q. Wu, and R. Q. Hu, "Resource allocation and trajectory design for MISO UAV-assisted MEC networks," *IEEE Transactions on Vehicular Technology*, Vol. 71, No. 5, 4933–4948, 2022.

[20] Zhang, Y., X. Hou, H. Du, L. Zhang, J. Du, and W. Men, "Joint trajectory and resource optimization for UAV and D2D-enabled heterogeneous edge computing networks," *IEEE Transactions on Vehicular Technology*, Vol. 73, No. 9, 13 816–13 827, 2024.

[21] Hu, X., K.-K. Wong, and Y. Zhang, "Wireless-powered edge computing with cooperative UAV: Task, time scheduling and trajectory design," *IEEE Transactions on Wireless Communications*, Vol. 19, No. 12, 8083–8098, 2020.

[22] Zhang, X., Y. Zhong, P. Liu, F. Zhou, and Y. Wang, "Resource allocation for a UAV-enabled mobile-edge computing system: Computation efficiency maximization," *IEEE Access*, Vol. 7, 113 345–113 354, 2019.

[23] Dai, X., Z. Xiao, H. Jiang, M. Alazab, J. C. S. Lui, S. Dustdar, and J. Liu, "Task co-offloading for D2D-assisted mobile edge computing in industrial internet of things," *IEEE Transactions on Industrial Informatics*, Vol. 19, No. 1, 480–490, 2023.

[24] Hu, X., C. Masouros, and K.-K. Wong, "Reconfigurable intelligent surface aided mobile edge computing: From optimization-based to location-only learning-based solutions," *IEEE Transactions on Communications*, Vol. 69, No. 6, 3709–3725, 2021.

[25] Qin, X., Z. Song, T. Hou, W. Yu, J. Wang, and X. Sun, "Joint optimization of resource allocation, phase shift, and UAV trajectory for energy-efficient RIS-assisted UAV-enabled MEC systems," *IEEE Transactions on Green Communications and Networking*, Vol. 7, No. 4, 1778–1792, 2023.